Äspö Hard Rock Laboratory

TRUE Block Scale project

**Stochastic continuum modelling
Model assessment and first
conditional model**

J. Jamie Gómez-Hernández
Harrie-Jan Hendricks Franssen

Technical University of Valencia (UPV)

February 1999

SKB

**Äspö Hard Rock
Laboratory**

Äspö Hard Rock Laboratory

TRUE Block Scale project

Stochastic continuum modelling Model assessment and first conditional model

J. Jamie Gómez-Hernández

Harrie-Jan Hendricks Franssen

Technical University of Valencia (UPV)

February 1999

Abstract

This report describes the implementation of a stochastic continuum model at the TRUE Block Scale site. The main objective during the building of this model was to assess whether such a model could be built conditional to the available data including geometrical data, material parameter data and pressure responses. After the assessment of the feasibility of such a model, a first model is built. The conclusion is that a stochastic continuum model can be built and the building process may help in understanding the role that the identified features play in the hydraulic behaviour of the site.

Sammanfattning

Denna rapport beskriver användandet av en stokastisk kontinuum-modell för True Block Scale-området. Huvudsyftet under uppbyggnaden av denna modell var att bestämma om den kan konditioneras på tillgänglig data i form av geometri, materialparameterar och tryckresponser. Efter fastställandet av genomförbarheten, konstrueras en första modell. Slutsatsen är att en stokastisk kontinuum-modell kan byggas och att processen kan bidra till att förstå vilken roll som de identifierade strukturerna spelar i platsens hydrauliska beteende.

Executive Summary

This report presents a stochastic continuum model of the True Block Scale site at a scale of hundreds of meters. The model consists of a lattice of cubic blocks discretizing a volume centred at the potential location of the tracer retention experiments.

The model has been built in a sequential manner. First the main structural features represented in the so-called October97 model, are used to classify the model blocks into fractured and non-fractured. Then, the material properties measured or interpreted at the boreholes are assigned to the corresponding discretization blocks. Later, within each fracture, the conductivity values are randomly generated using a conditional stochastic simulation approach in which spatial correlation is accounted for and measured values are honoured. Finally, the resulting 3-D heterogeneous block of conductivities is perturbed until, first, the undisturbed heads and, second, the transient pressure responses, observed in the boreholes are matched by the results of the numerical simulation of steady-state and transient flow within the simulation block. For the latter step, boundary conditions are necessary, which are taken from the regional model of the site.

The above procedure can be repeated for several realisations for which the classification into fractured/non-fractured blocks remains unaltered, but the block conductivity distribution varies from one realisation to another. The process is computer intensive and only one realisation is presented and discussed.

After assessing the feasibility of such a model, the September98 structural model together with the results from the interference tests carried out during the spring of 1998 were used to built a first conditional model fully based on quantitative data.

The main conclusion of this work is that a stochastic continuum model conditioned to all the information described above can be built. The sequential nature of the conditioning process helps in understanding the implications that the observed pressure responses have in the conductivity of the different fractures. It may also help in detecting the need of including additional fractures in the structural model in order to achieve the best reproduction of the observed pressure data.

Contents

List of Figures

List of Tables

1   Introduction

The purpose of this report is twofold, first it demonstrates the capabilities of a stochastic continuum approach for flow modelling of fractured media in the context of the True Block Scale experiment, then, it presents an application to the True Block Scale site using the data from the spring 1998 interference tests. Stochastic continuum modelling of a fracture site is especially attractive for the easiness in which different types of information regarding geometry, material properties and pressure response can be brought into the model. Incorporating the different types of information is done in a sequential manner that permits the analysis of the influence of the additional information on the material properties and flow behaviour of the block. In addition, the stochastic nature of the approach allows the analysis of the uncertainty associated to the imperfect knowledge of the medium being modelled.

The report is organised in two distinct sections, in the first section the feasibility of the proposed model is assessed using the October97 structural model and some qualitative information on pressure propagation in the block derived from the log of activities during the simultaneous drilling of KA2563A and KA3510A. In the second section, a first model is built based on the September98 structural model and conditioned to six of the interference tests carried out during the spring of 1998.

2   Model assessment

In this first section, an assessment of the possibilities of stochastic continuum modelling by the self-calibrated model is carried out. At the time this assessment was done, the October97 structural model represented the current understanding of the geology in the modelling area; however, the hydraulic information available in the area of study had been collected as part of the logging activities during the drilling of the boreholes, but no explicit interference testing had been performed. The aims of this preliminary modelling work are:

- to establish a suitable modelling area, large enough for the later modelling of the tracer tests and with a discretisation as fine as it could be handled by the available computer code

- to evaluate the feasibility of the self-calibrated algorithm in a three-dimensional model with multiple fractures and conditional to steady-state and transient piezometric heads

- to gain a preliminary understanding of the hydraulic functioning of the block in the surroundings of the potential tracer test area.

2.1   Model geometry

The model geometry used during the model assessment phase is based on the October97 structural model by Hermanson (1998a) and it is slightly different from the model geometry used in the next chapter which benefits from additional hydraulic data and a re-evaluation of the structural model.

2.1.1   Discretisation

The area modelled has an extension of 247 m by 227 m by 287 m and is discretized into 37 by 34 by 43 cubic cells of 6.67 m size. The modelled area has been chosen so that all five main boreholes (KA2563A, KA2511A, KA3510A, KI0025F and KI0023B) are completely contained within it. (Borehole KI0025F02, built later, is also included within the model domain). It extends from 1790 m to 2037 m West to East, from 7050 to 7277 South to North, and from –570 m to –283 m bottom to top.

2.1.2   Fractures

All fractures are included deterministically in the model. For this purpose, each fracture is assimilated to a plane which is overlaid on the discretized model. Each of the model cells that is intersected by one of the fracture planes is classified as fractured. The remaining cells are classified as non-fractured. The twenty fractures described in the technical report by Hermanson (1998a) have been used for this classification. As a result, 44% of the more than 50,000 cells are intersected by a fracture plane, and 56% are not. The non-fractured cells should not be interpreted as representing the rock matrix but as representing an equivalent medium including the rock matrix and the background fracturing that is not explicitly included in the structural model.

Figure 2-1 and 2-2 show the three-dimensional mask identifying the cells intersected by all fracture planes. Figure 2-1 shows the intersections of the fracture planes with the faces of the model block and Figure 2-2 shows several slices of the 3D mask. The fracture planes, as it can be appreciated in the figures, extend all the way to the sides of the block, therefore, enhancing the connectivity implied by the shorter lengths assigned to the fractures in the October97 model by Hermanson (1998a). This connectivity will be corrected during the process of pressure conditioning by local modifications of the conductivity values of the cells on the fracture planes.
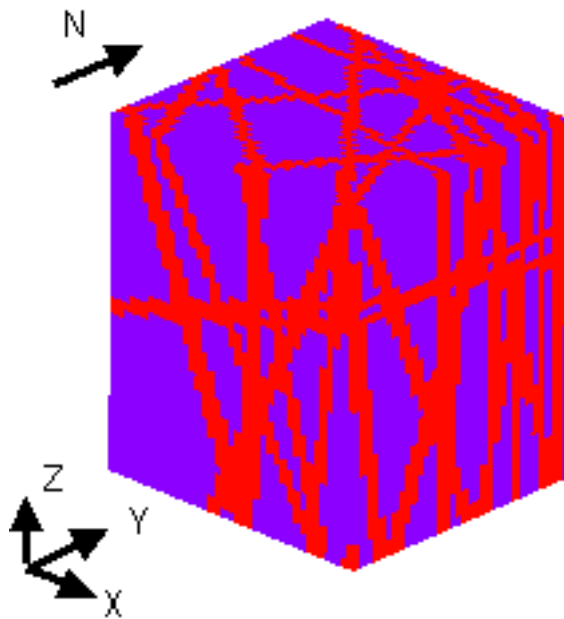
Figure 2-1. *Block mask showing the intersection of the fractures with the block faces. Based on the October97 structural model (Hermanson, 1998a).*

| *Level 2 (-556 m)* | *Level 6 (-530 m)* | *Level 16 (-463 m)* |
| *Level 26 (-396 m)* | *Level 36 (-330 m)* | *Level 43 (-283 m)* |
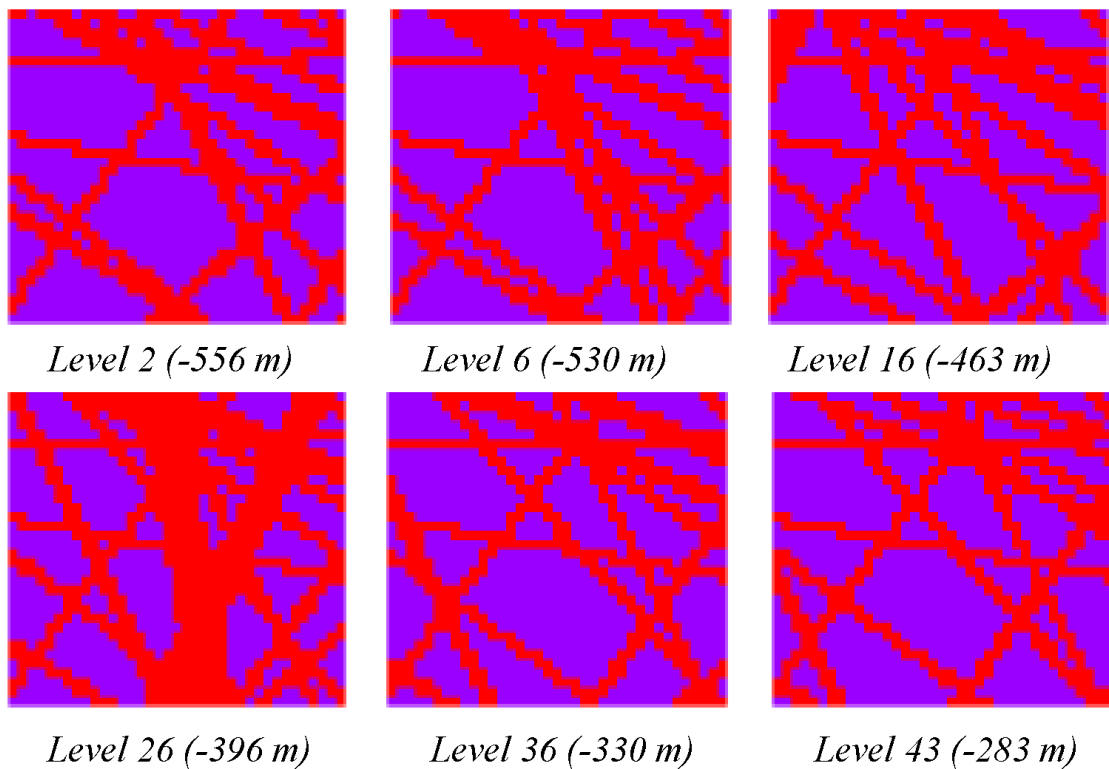
Figure 2-2. *Horizontal slices of the block in Figure 2-1.*

2.2   Material properties

Transmissivities are assigned to each of the individual fractures independently. For each fracture, a conditional realisation of conductivities drawn from a multi-lognormal distribution is generated. The conditioning values are derived from the transmissivities measured in the steady state 5 m double packer flow logging, which, in turn were obtained by Moye's formula (Gentzschein, 1997a,b; 1998). This flow log provides conditioning data at 21 fractured cells and at 101 non-fractured cells. Their values are listed in Appendix 1.

The average logconductivity of the non-fractured cells is -10.2 $\log_{10}$ m/s and the variance is 1 $\log^2_{10}$ m/s, whereas in the fractured cells, the average is -6.5 $\log_{10}$ m/s and the variance 0.5 $\log^2_{10}$ m/s.

There were not enough data to compute variograms, therefore, an isotropic spherical variogram was postulated with a range of 40 m. The range was chosen to introduce some continuity within the modelling block but short enough to allow for some heterogeneity in the fracture planes. This range will also plays a role during the phase of conditioning to piezometric heads, its value is reasonable to allow the fractures to be locally perturbed to achieve conditioning. Sensitivity tests to the presence of anisotropy

and to the variogram range were not performed since the objective of this part of the work was to show the possibility to build a stochastic continuum model of a fractured media conditional to conductivity and piezometric head data.

During the calibration to the transient information, a constant storativity coefficient was used and equal to 2.0E-05. This value was chosen based on our experience from models in similar media and from the response times observed in the interferences observed during drilling.

2.3   Flow simulations

The solution of the groundwater flow equation is obtained by standard seven-point block-centred finite differences using the geometric mean of adjacent cells to compute the intercell conductivities. The solution of the finite-difference linear system of nearly 50,000 equations is obtained by biconjungate preconditioned gradient with incomplete LU decomposition (Greenbaum, 1996). This method takes optimal advantage of the sparse nature of the conductance matrix and allows to handle the large conductivity contrasts that appear between adjacent cells. The conductance matrix is, in any case, highly unstable and some implementation refinements had to be performed in order to ensure convergence.

For the steady-state simulation, prescribed head values along the six faces of the parallel-piped are imposed. The values used were taken from the regional model by Svensson (1997). They impose an average gradient towards the tunnel galleries of about ten percent. In conjunction with the values taken from the regional model, the cells of the model block that were intersected by the tunnel are assigned a piezometric head corresponding to atmospheric pressure. A view of the prescribed heads on three of the faces of the parallel-piped is given in Figure 2-3.
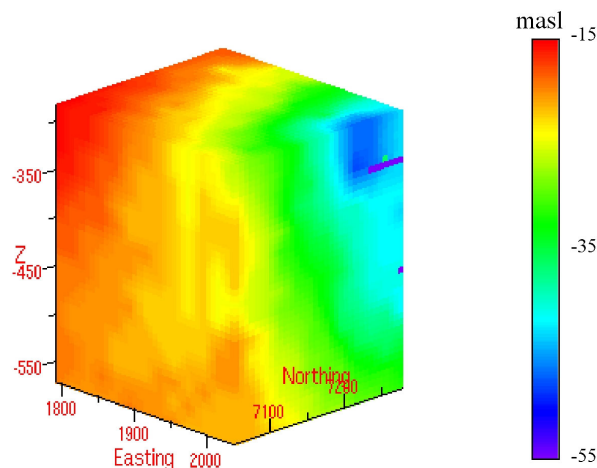
Figure 2-3. *Prescribed heads used as boundary conditions in m used for the solution of the groundwater flow equation. Tunnel cell values are outside the colour scale.*

2.4   Conditioning to measured piezometric heads

The realisation of the conductivity field generated as discussed in section 2.2 will not, in general, reproduce the observed heads at the monitoring locations when the flow equation is solved using the boundary conditions of Figure 2-3. In order to condition the conductivity realisation to piezometric heads the self-calibrated algorithm is used (Gómez-Hernández et al., 1997), a perturbation conductivity realisation is computed that added to the seed realisation results in a new realisation in which the solution of the flow equation matches the measured piezometric heads. The perturbation is computed by non-linear optimisation. The details of the calculation can be looked up in the previously referred to paper, although the technique is outlined in Appendix 2.

Besides its fundamental objective of producing realisations conditional to both transmissivity and head measurements, the self-calibrated algorithm allows monitoring of the impact that the conditioning data has in the spatial distribution of conductivities. First, a realisation is generated conditional to only conductivity data, then, the realisation could be made conditional to steady-state heads, then it can be made conditional to transient heads including one or several interference tests. During the conditioning process, the evolution of the conductivity realisation can be monitored and some considerations could be made about the implications that the observed pressure responses have in the inner connectivity of the block.

Figure 2-4 shows a conductivity field built by merging the realisations of hydraulic conductivities on the 20 fracture planes with the generated background conductivity distribution corresponding to the non-fractured cells into the a single block. As previously mentioned, this realisation is conditional to the 132 measured logconductivity data values but does not take into account the piezometric head information. This field is referred to as the seed field.

The so-called undisturbed piezometric heads measured at a number of borehole sections were considered as measured under a steady-state situation and were then used to condition the seed field in Figure 2-4. The values used and their co-ordinates are given in meters in Table 2-1 with their co-ordinates referred to the origin of the model block. The application of the self-calibrated algorithm to the seed field in Figure 2-4 results in a new field in which the solution of the flow equation yields the set of conditioned heads provided in the last column of Table 2-1. As it can be seen in Figure 2-5 the conditioned field almost reproduces exactly the observed undisturbed values.

Table 2-1 . Undisturbed piezometric head values used as conditioning data. Co-ordinates are in Äspö local system. Last column shows the piezometric heads resulting from the solution of the flow equation in the conditioned conductivity field

x (m)	y (m)	z (m)	Observed heads (m)	Conditioned heads (m)
1869.9	7109.1	-455.3	-27.4	-27.9
1915.2	7140.1	-419.1	-30.7	-30.7
1958.1	7170.3	-383.1	-31.5	-31.5
1990.7	7192.7	-358.3	-35.4	-35.5
1940.3	7074.5	-499.1	-24.8	-24.8
1942.1	7088.7	-494.5	-25.1	-25.1
1946.7	7126.5	-482.5	-26.7	-26.7
1951.3	7163.3	-470.5	-28.1	-28.2
1954.1	7185.9	-462.7	-35.4	-34.9
1958.9	7224.7	-449.1	-38.1	-38.2
1830.7	7157.7	-539.5	-26.5	-26.6
1901.9	7198.3	-469.3	-28.9	-28.5
1912.7	7204.7	-459.9	-28.0	-28.6
1927.3	7213.1	-445.3	-32.2	-32.7
1963.1	7234.7	-408.3	-39.2	-39.6
1913.7	7181.7	-471.5	-30.3	-28.9
1917.7	7187.1	-469.1	-28.3	-28.9
1921.1	7192.7	-466.5	-28.7	-29.0
1928.7	7204.1	-461.3	-29.9	-29.9
1936.5	7215.5	-455.5	-35.7	-34.9
1946.7	7230.7	-448.9	-47.7	-47.9

Figure 2-6 shows the field of perturbations that have to be applied to the block in Figure 2-4 to achieve conditioning to the steady-state head values. In this figure one can appreciate how the conductivities in some fractures are increased whereas in some others they are decreased. These perturbations do not necessarily have to be uniform throughout the entire fracture plane, although in this particular case the shift of conductivities is quite homogeneous in each fracture.

Figure 2-7 shows a number of horizontal cross-sections of the simulated steady-state heads solution of the groundwater flow equation in the model block. Remember that the heads on all four sides of all sections were prescribed as given in Figure 2-3.
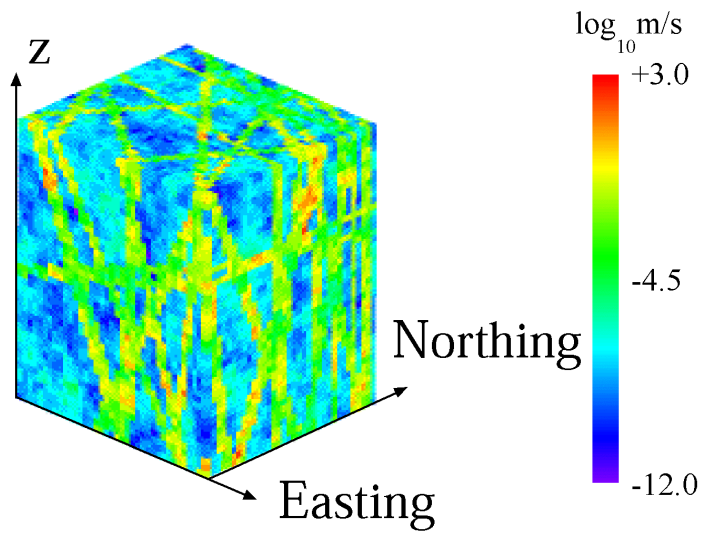
Figure 2-4. *Three-dimensional isometric view of the seed logconductivity realisation. Scale is in log$_{10}$m/s.*
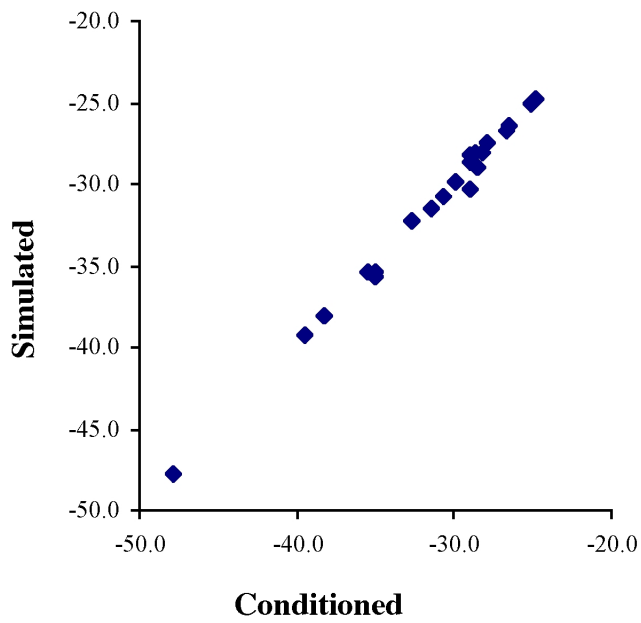
Figure 2-5. *Degree of conditioning to the steady-state heads achieved by the self-calibrated approach after perturbing the seed field in Figure 2-4 .*

2.5   Conditioning to transient heads

The next step was to test the ability of the self-calibrated algorithm to condition the conductivity realisation to transient piezometric head data in a three-dimensional fractured block. The only transient information available at this stage was from the compilation of activities during the drilling of some boreholes. More precisely, we used the pressure responses to the simultaneous drilling of boreholes KA2563A and KA3510A reported by Hermanson and Follin (1997). Given that all the information necessary to attempt to reproduce these drillings as if they were interference tests was not available, only information about the type of responses observed when the boreholes reached certain fractures was collected from this report and imposed on the conductivity field. More precisely, noticeable responses are observed in the four monitoring sections at KA3511A when borehole KA3510A hits fracture 5 at a depth of 47 m and when borehole KA2563A hits fractures 4 (at 94 m depth), 5 (at 103 m depth) and either/both 6/7 (at 153 m depth). Not any other significant response was observed when either borehole crossed any other fracture.
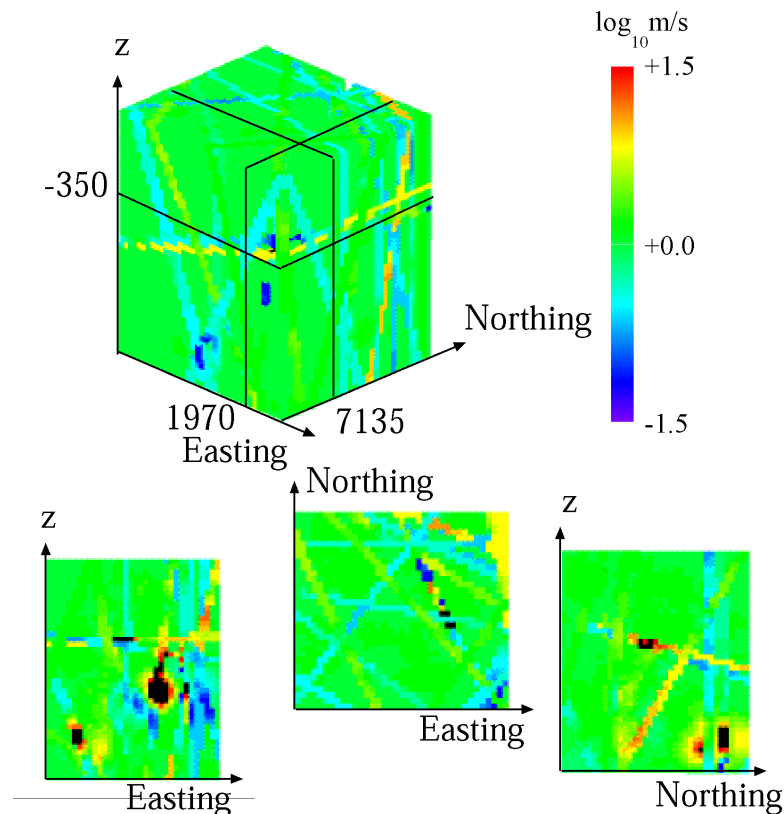
Figure 2-6. *Perturbation applied to the logconductivity realisation in Figure 2-4 in order to achieve conditioning to the steady-state head conditioning data in Table 2-1*
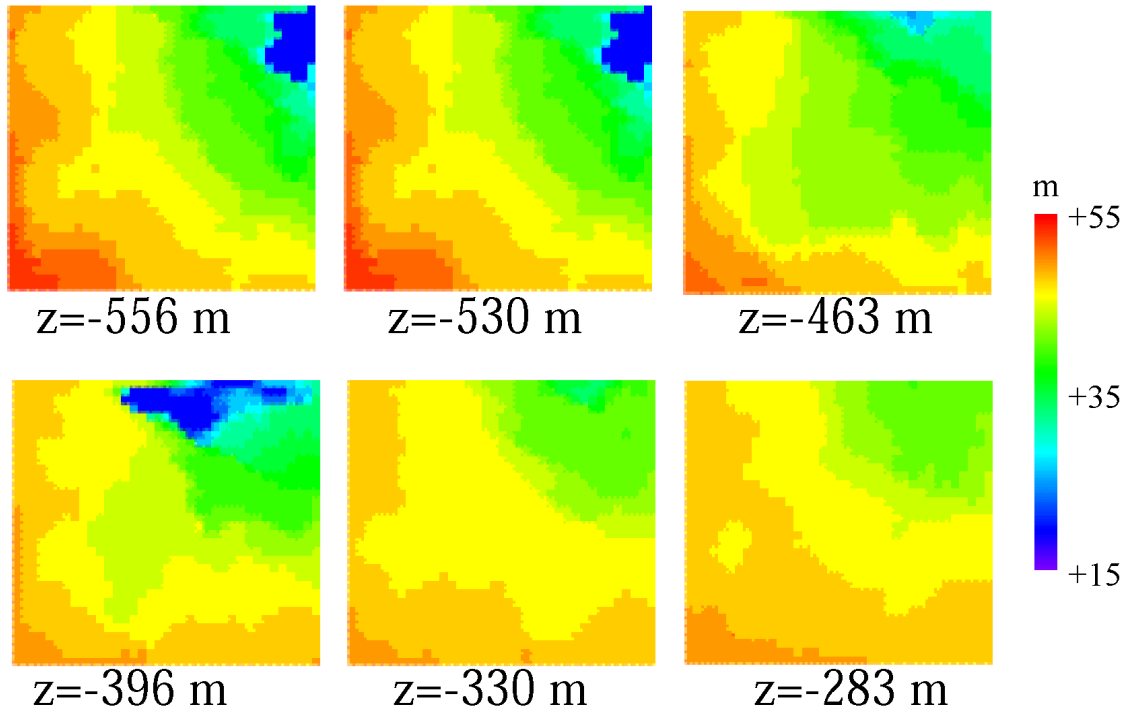
Figure 2-7. *Horizontal slices of the steady-state head solution on the conditional*
logconductivity field obtained after perturbing the one of Figure 2-4

The above behaviour was translated into transient conditioning information as follows:
when an atmospheric pressure pulse travels through the block along the traces of wells
KA3510A and KA2563A at a speed of 6 m/d (roughly one discretisation cell per day)
pressure responses should be observed in borehole KA3511A with the same pattern
observed during the drilling. Notice that the actual boundary conditions that would
correspond to drilling are more complex than simply lowering the pressure at which the
drilling head is located down to atmospheric pressure.

Figure 2-8 shows a horizontal slice at z = –472 m—corresponding to the intersection of
borehole KA3510A, at 47 m depth with fracture number 5—of the simulated
drawdowns at the moment that the pressure pulse has been at that location for 8 hours.
Three displays are shown, the first one corresponds to the simulation in the seed
logconductivity field of Figure 2-4, the second one in the logconductivity field
conditioned to steady-state heads, and the last one in the logconductivity field
conditioned to both steady-state heads and the transient head information. It is clear how
only after conditioning to the transient information the propagation of the pulse along
fracture 5 is achieved.

Seed field   Steady-state conditioned Transient conditioned
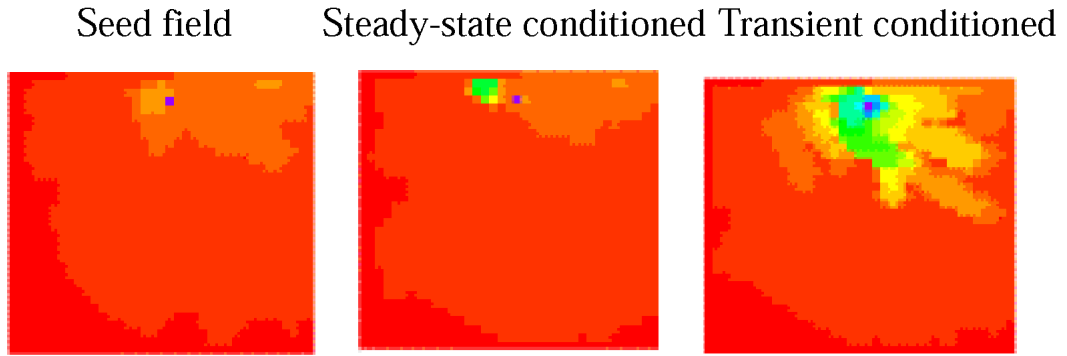
Figure 2-8. *Horizontal slices of the drawdowns simulated in the seed field of Figure 2-4, in the conductivity field conditional to steady-state heads and in the conductivity field conditioned to the transient information. The slice is taken at z=-472 m which correspond to the intersection between borehole KA3510A and fracture number 5 and at the time that the pressure pulse that is traveling down-the-hole has reached this plane.*

Figures 2-9 to 2-11 show similar results to Figure 2-8 but corresponding to the instants in which the pressure pulse along borehole 2563A intersects fracture number 4 (at 94 m depth), then fracture number 5 (at 103 m depth) and then fractures 6 and 7 (at 153 m depth).

Seed field   Steady-state conditioned Transient conditioned
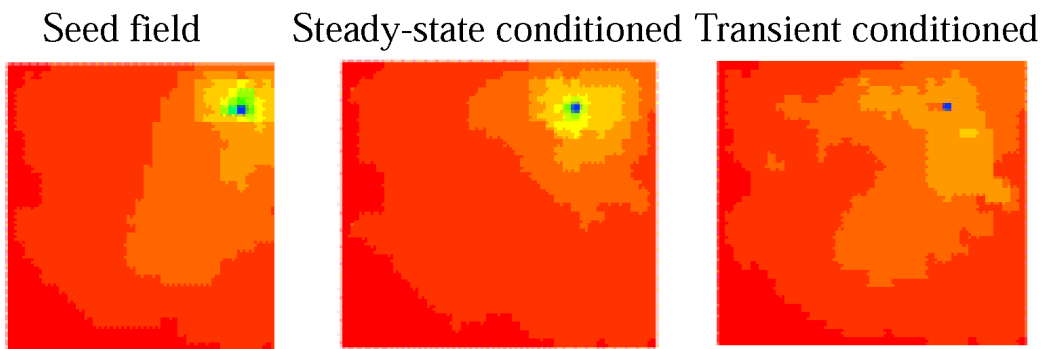
Figure 2-9. *As in Figure 2-8. The slice is taken at z=-404 m which correspond to the intersection between borehole KA2563A and structure number 4 and at the time that the pressure pulse that is travelling down the hole has reached this plane.*

Seed field   Steady-state conditioned Transient conditioned
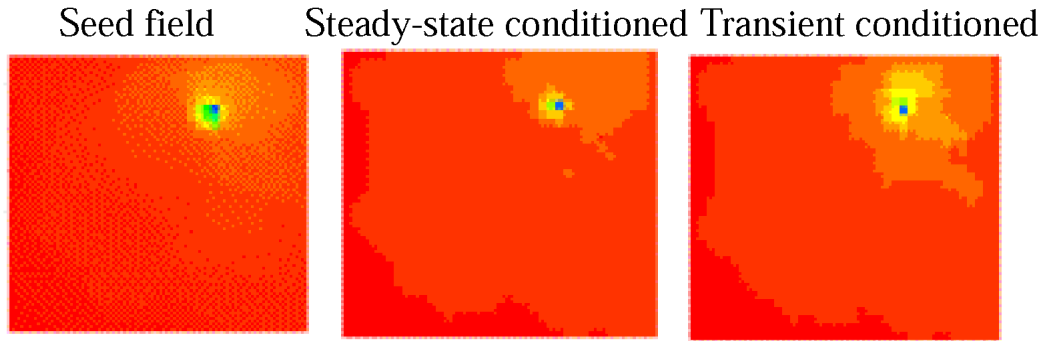
Figure 2-10. *As in Figure 2-8. The slice is taken at z=-410 m which correspond to the intersection between borehole KA2563A and fracture number 5 and at the time that the pressure pulse that is travelling down the hole has reached this plane.*

Seed field   Steady-state conditioned Transient conditioned
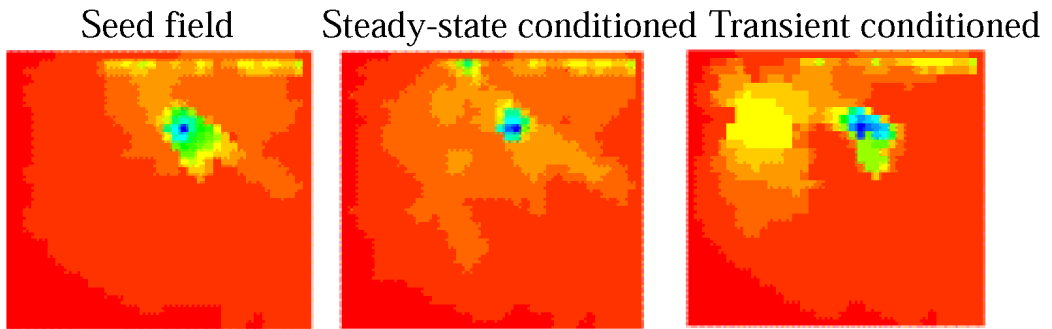
Figure 2-11. *As in Figure 2-8. The slice is taken at z=-443 m which correspond to the intersection between borehole KA2563A and structure number 5 and at the time that the pressure pulse that is travelling down the hole has reached this plane.*

The final conditioned logconductivity field matches the conductivity data at the measurement locations, reproduces the undisturbed heads where they had been reported and has a transient response coherent with the log of events reported during the simultaneous drilling of boreholes KA3510A and KA2563A.

The conclusion from this assessment phase is that it seems possible to build a hydraulic model of the site at the 250 m scale using the stochastic continuum concept. However, it seems difficult the possibility of constructing an ensemble of realisations that could be used for the analysis of uncertainty in flow (and transport) predictions, due to the large amount of computer power needed to generated each of the conditional realisations. The work described up to here presents the generation of a single conditional realisation, multiple realisations should be generated conditional to the same information to reinforce the conclusions that are drawn on the basis of this individual realisation.

3 Conditional model

After the data from the cross-hole tests performed during the spring of 1998 was available, the next objective is to build a logconductivity model of the block of interest conditioned to this transient information which is more of a quantitative nature than the one used during the model assessment phase.

The aims of this phase are:

- to produce realisations of logconductivity conditional to the available logconductivity and interference test data

- to analyse, during the conditioning process, how the logconductivity realisation evolves

- to draw some conclusions about the importance of some fractures in the hydraulic behaviour of the block

3.1 Model geometry

The model geometry is virtually the same as the one used during the model assessment phase described in section 2. The only (and important) difference regards the fractures included since a new structural model was available. The September98 model (Hermanson, 1998b) benefits, with regard to the October97 model, of the information gathered after the drilling of borehole KI0023B, of additional hydraulic test information and of important interaction between structural geologists and hydrogeologists. Besides small changes in the geometry of all fractures, the main difference between the two structural models is the inclusion of fracture number 13 which runs more or less parallel between fractures number 19 and 20 and which could play an important role in the envisaged tracer experiment. Figure 3-1 displays the new three-dimensional block mask showing the intersection of all fractures with the faces of the model block. Comparison to Figure 2-1 shows the differences between the two structural models.

The material properties are the same as in the model assessment phase, that is, the same logconductivity conditioning data listed in Appendix 1 and the same statistics are used for the generation of the conditional realisations of each individual fracture, once each fracture has been generated, they are all merged together on a three-dimensional realisation together with the non-fractured blocks.

3.2   Flow simulations

The flow simulations are carried out using the same numerical scheme as in the model assessment phase. The same set of prescribed heads described in 2-3, taken from Svensson (1997) model, are used for the simulation of steady-state conditions.

For the simulations of the interference tests, the heads on the six faces of the model block were set to zero and only drawdowns are simulated.
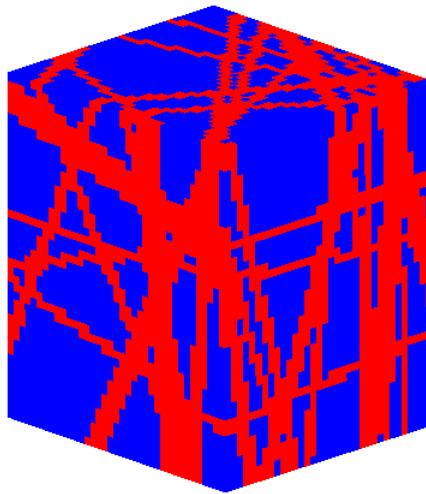
Figure 3-1. *Three-dimensional block mask showing the cells that are modelled as fractured blocks. Based on the September98 structural model (Hermanson, 1998b)*

3.3   Conditioning to the interference tests

The objective of this phase is to build a logconductivity model based on a seed field generated according to the material properties listed above and with the distribution of fractures depicted in Figure 3-1. The initial intention was to build directly a realisation conditional to all nineteen cross-hole interference tests (Andersson et al., 1998); however, after the first tests, the task was beyond our computer capabilities. A decision was taken to select a subset of the interference tests and condition, initially, only to these tests. The attempt to condition to a subset of 7 tests, six short-term and a long-term one, in a single step was not viable: the conditioning step, which involves a heavy optimisation, did not converge, partly because of conflicting objectives from the difference cross-hole tests. The solution was to include the tests sequentially, so that a logconductivity field is made conditional to the cross-hole tests in increasing succession: a seed field is used to obtain a logconductivity field conditional to one short-term test, the resulting field is used as a seed field to generate a new one conditioned to the previous short-term test plus an additional test, and so on. Following this procedure it was possible to generate the logconductivity field of Figure 3-2 conditional to the tests

listed in Table 3-1. Table 3-2 gives the monitoring head locations used in the conditioning process. The selection of the tests was done with the following criteria: tests #7 and 8 were chosen because they seemed to be easy to reproduce, matching them involves mostly making less permeable some of the fractures that were originally too connected in space (test #7 also tests fracture #7 that could be a downstream boundary for the tracer test modelling); tests #9 and 12 focused on fracture #19 one of the possible bounding features of the tracer tests domain; test #13 had significant responses in several locations, and test ESV-1c had been used for tracer testing and we wanted to make some contaminant transport tests using the data from this tracer test on a conductivity field already conditioned to the flow response.
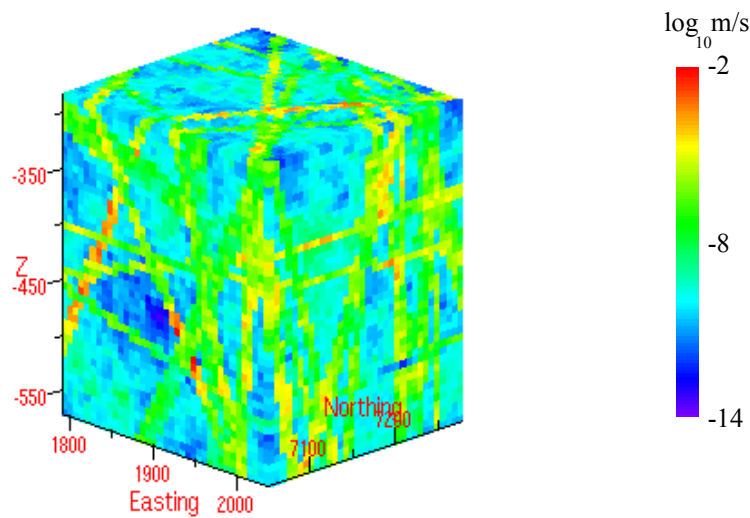
Figure 3-2. *Logconductivity field conditioned to the interference tests in Table 3-1. Scale in log_{10} m/s*

The process of conditioning to the piezometric heads is carried out using a non-linear optimisation algorithm. As opposed to the standard geostatistical conditioning, conditioning through optimisation does not ensure exact reproduction of the conditioning data. Figure 3-3 shows the degree of reproduction of the monitored piezometric heads for each one of the six interference tests included. As it can be appreciated, the reproduction of the measured heads is not as good as desired especially for test ESV-1c. The use of tests #7, 8 and 12 in which the measured responses are either null or negligible helped in reducing some of the existing connectivity in the seed logconductivity field. In these three tests, the seed conductivity field had several sections with simulated responses that after conditioning show no response. The most significant mismatches occur for test ESV-1c particularly with regard to fracture #20: two of the sections that show good response in the field intercepted by fracture #20 are not being matched in the simulation. Increasing the conductivity of this fracture does not improve the match while it introduces too large discrepancies in the reproduction of test #8. There is a need to connect the source section to section #20. On the other hand the response at the source location and in sections P4 and P5 of KI0023B are very well reproduced.

15

Table 3-3 shows the evolution with conditioning of some statistics computed for each fracture. Notice that all fractures start with mean values of logconductivity around −6.5 $\log_{10}$m/s and some of them suffer important changes during the process of conditioning to piezometric heads. Most noticeably, fracture #5 increases its conductivity almost two orders of magnitude, and fracture #7 decreases its conductivity one and a half order of magnitude. With regard to the fractures close to the envisaged area for the tracer test, the most important change occurs in fracture #19 that increases its average conductivity almost by an order of magnitude. The histograms of logconductivity in the fractures evolve from close to Gaussian to negatively skewed with the net effect of an increase of within fracture heterogeneity. The fractures in which this effect is most noticeable are numbers 7, 8, 9 and 20. This negative skewness which is produced by the appearance of cells with conductivities in the order of magnitude of the non-fractured cells could be understood as a correction to the enhanced connectivity introduced in the seed logconductivity field, in which all fractures are incorporated as planes extending to the limits of the model block.

Table 3-1. Interference tests to which the logconductivity field of Figure 3-2 is conditioned

| Test #	Type	Source	Flow period (h)	Model cell for source	Fracture being tested
7	CH[1]	KI0025F:R3	0.5	(24, 11, 13)	?
8	CH	KI0025F:R5	0.5	(25, 20, 16)	#6, #7
9	CH	KI0025F:R2	0.5	(23, 6, 11)	#19
12	CH	KI0023B:P2	0.5	(17, 17, 13)	#19
13	CH	KA3573A:P1	0.5	(16, 33, 20)	#15
ESV-1c	CQ[2]	KI0023B:P6	384.0	(20, 21, 15)	#9

[1]Constant head test, [2]Constant flow test

Table 3-2. List of locations used to monitor piezometric heads during the interference tests in Table 3-1 and employed for the conditioning to the logconductivity field of Figure 3-2

Monitoring location	Cell in model	Information provided
KI0025F:R1	(23, 4, 11)	Response observed during test #9
KI0025F:R2	(23, 6, 11)	Imposed head drawdown during test #9
KI0025F:R3	(24, 11, 13)	Imposed head drawdown during test #7, response observed during tests #9 and ESV-1c
KI0025F:R4	(24, 17 ,15)	Response observed during tests #7 and ESV-1c
KI0025F:R5	(25, 20, 16)	Imposed head drawdown during test #8, response observed during test #13
KI0025F:R6	(25, 26, 18)	Response observed during test #13
KA2511A:S2	(12, 9, 17)	No response observed in any test
KA2511A:S3	(19, 14, 23)	No response observed in any test
KA2511A:S4	(25, 18, 28)	No response observed in any test
KA2511A:S5	(30, 21, 32)	No response observed in any test
KA2563A:R1	(6, 16, 5)	Response observed during test ESV-1c
KA2563A:R4	(17, 22, 15)	Response observed during test ESV-1c
KA2563A:R5	(18, 23, 16)	Response observed during test ESV-1c
KA2563A:R6	(21, 25, 19)	Response observed during test ESV-1c
KA2563A:R7	(26, 28, 24)	No response observed in any test
KI0023B:P4	(19, 20, 15)	Response observed during test ESV-1c
KI0023B:P5	(19, 21, 15)	Response observed during test ESV-1c
KI0023B:P6	(20, 21, 15)	Source location for test ESV-1c
KI0023B:P7	(21, 23, 16)	Response observed during test ESV-1c
KI0023B:P8	(22, 25, 17)	Response observed during test #13
KI0023B:P9	(23, 27, 18)	Response observed during test #13
KA3510A:P1	(16, 30, 14)	No response observed during any test
KA3573A:P1	(16, 33, 20)	Imposed head drawdown test #12
KA3573A:P2	(16, 30, 19)	Response observed during test #12
KA3600F:P1	(11, 34, 20)	No response observed during any test
KA3600F:P2	(7, 33, 20)	Response observed during test #12

Figures 3-4 and 3-5 show horizontal cross-sections of the final conditioned logconductivity field and of the perturbations applied to the seed field in order to arrive at the conditional field. These figures indicate that the perturbations are quite significant especially in the levels around –450 m. On one hand the contrast becomes fractured and non-fractured cells increases, and on another some of the fractures become very conductive, such as are fractures #8 and 19. Figure 3-6, 3-7 and 3-8 show the final logconductivity distributions in fractures #8, 19 and 20 along with the perturbation applied to the seed logconductivity field in order to arrive at the conditional realisation.
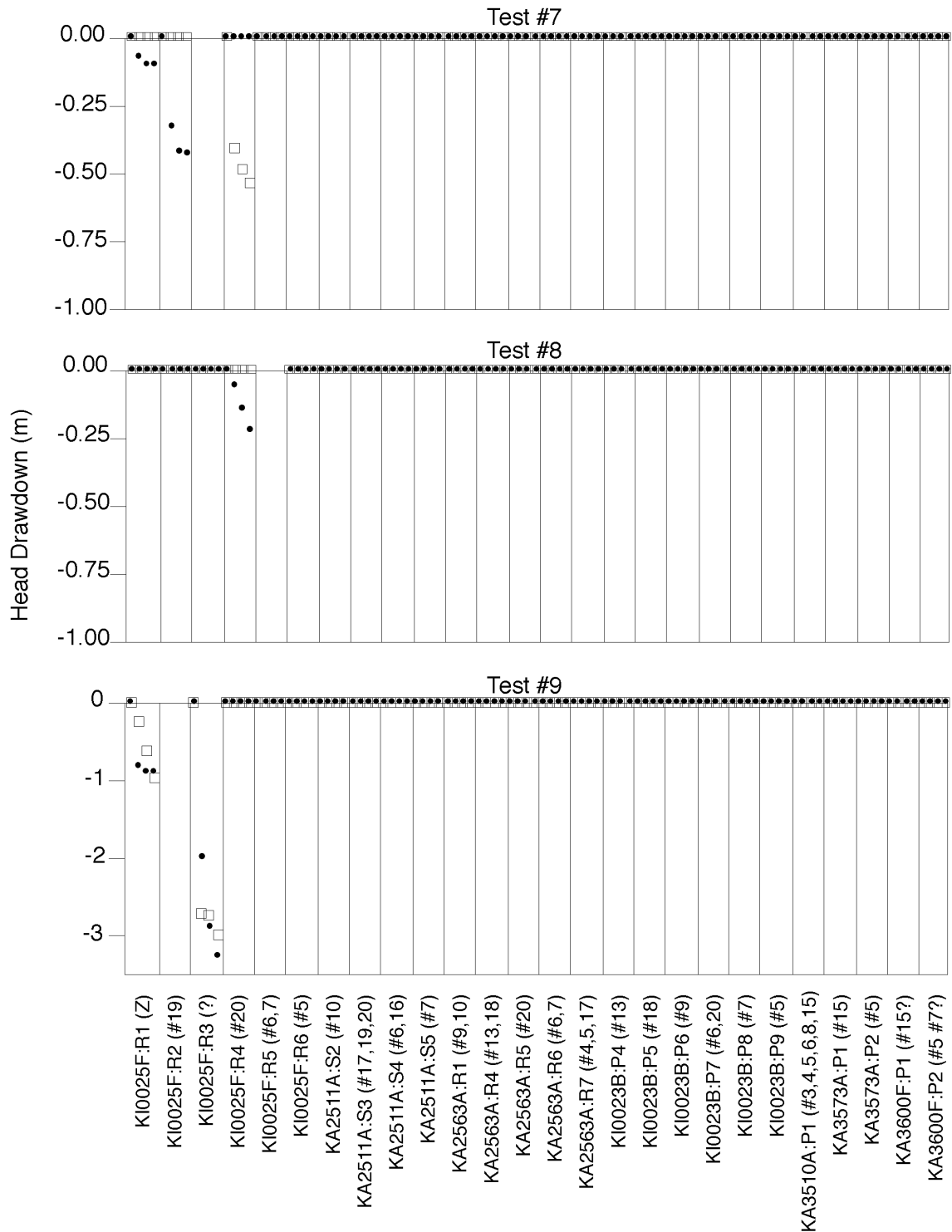
Figure 3-3. *Reproduction of the observed heads in the logconductivity realisation after conditioning. The squares represent the measurements, the dots, the simulated values. If the dots are inside the square the conditioning process was satisfactory. All 26 observation locations are displayed. Each vertical bar represents 0.5 hours except for test ESV-1c for which each bar represents 384 hours. Notice the variation of the scale of the head drawdown axis.*

18
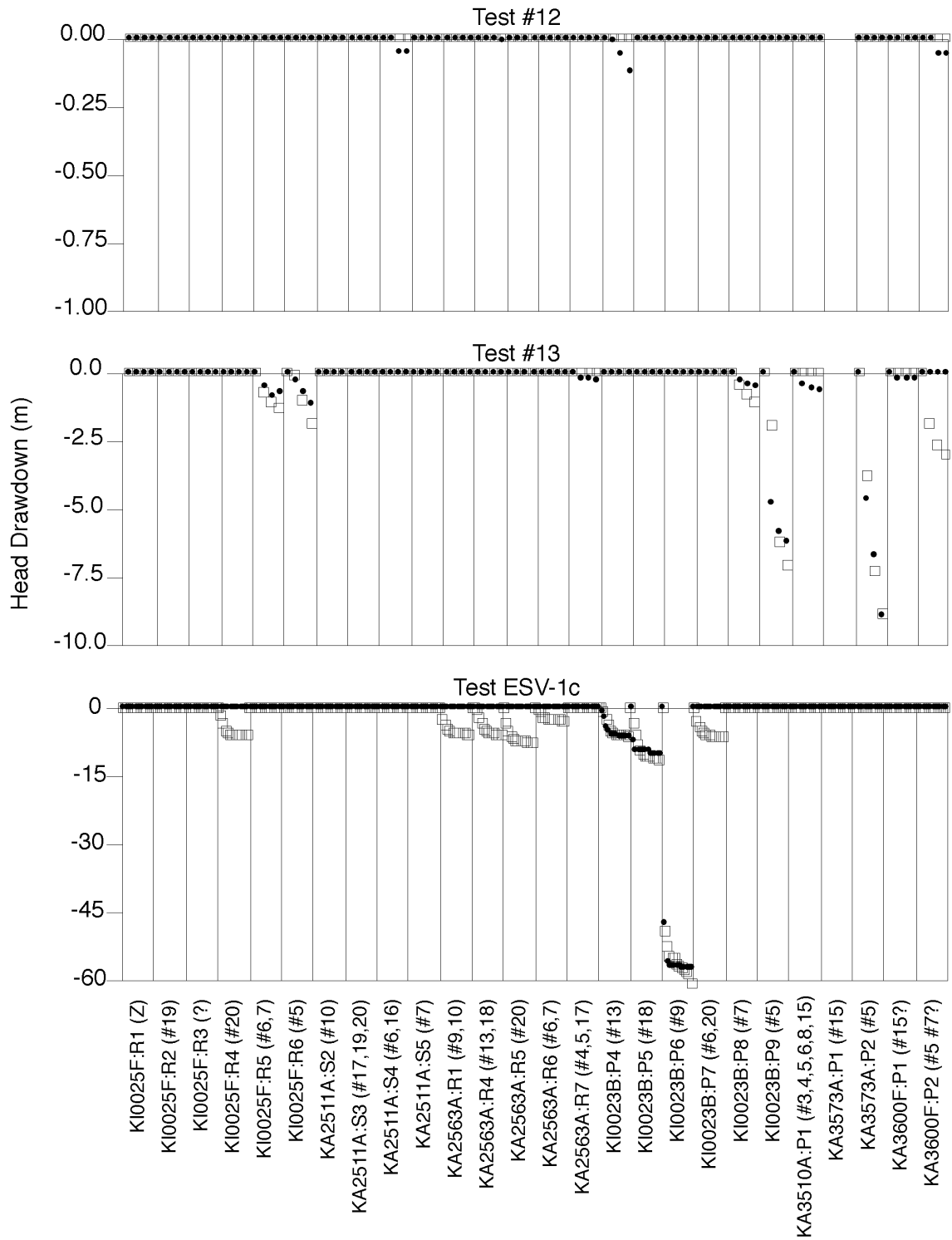
Figure 3-3. (Cont.)

Figures 3-6 to 3-8 permit to appreciate the need for local heterogeneities within the fracture planes in order to match the measured piezometric heads. Locally the fractures planes must contain areas of high and low conductivities. This heterogeneity could be interpreted as heterogeneity in fracture aperture. It is also interesting to note how some fracture intersections are clearly distinguishable within the fracture planes due to their conductivity contrast with the rest of the fracture planes, whereas some others remain camouflaged on the fracture plane.

Table 3-3. Evolution of fracture average conductivities as piezometric head information is used in the conditioning process

Fracture	Average fracture values on seed realisation	Average fracture values on realisation conditioned to steady-state head	Average fracture values on realisation conditioned to transient piezometric heads	Average change on fracture conductivity between the seed realisation and the one conditioned to transient heads
Background	-10.12	-9.83	-10.19	-0.07
#1	-6.47	-6.54	-6.54	-0.07
#2	-6.32	-6.22	-6.34	-0.02
#3	-6.47	-6.40	-6.46	+0.01
#4	-6.44	-7.30	-7.32	-0.88
#5	-6.55	-4.98	-4.62	+1.93
#6	-6.75	-8.18	-8.29	-1.54
#7	-6.39	-7.27	-7.37	-0.98
#8	-6.41	-4.78	-5.38	+1.03
#9	-6.56	-8.05	-8.02	-1.46
#10	-6.29	-7.57	-7.41	-1.12
#11	-6.55	-7.93	-7.77	-1.22
#13	-6.48	-6.55	-6.59	-0.11
#15	-6.51	-7.75	-7.59	-1.28
#16	-6.27	-5.42	-5.32	+0.95
#17	-6.28	-6.19	-5.90	+0.38
#18	-6.22	-6.77	-7.04	-0.82
#19	-6.40	-5.98	-5.52	+0.88
#20	-6.44	-6.35	-6.58	-0.14
#Z	-6.30	-7.20	-7.13	-0.83
EW-1	-6.30	-6.33	-6.32	-0.02

z = -550 m   z = -450 m   z = - 350 m
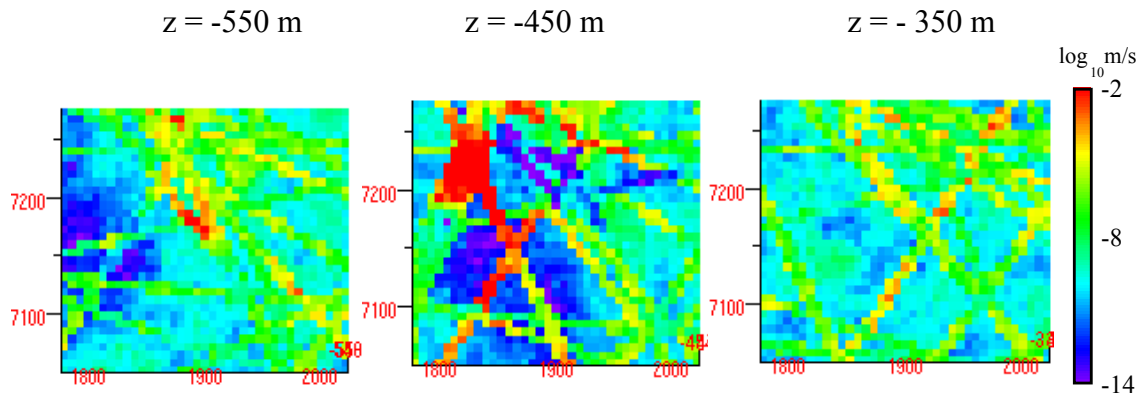
Figure 3-4. *Three horizontal cross-sections of the final conditional logconductivity block in Figure 3-2*

z = -550 m   z = -450 m   z = - 350 m
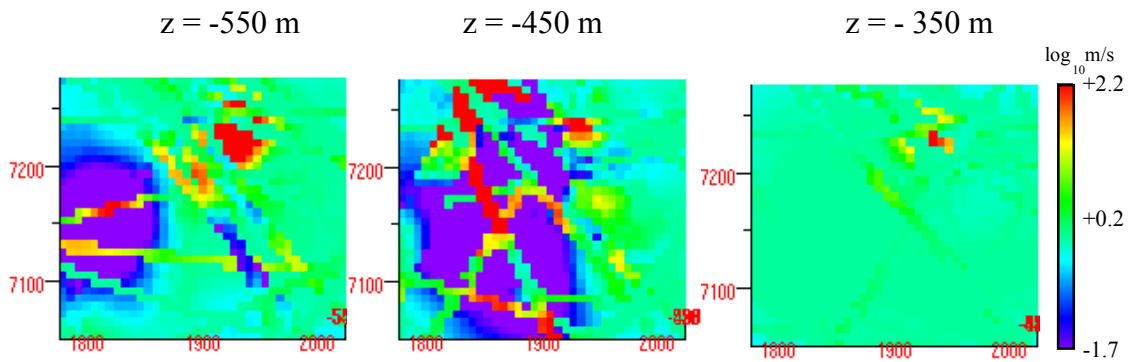
Figure 3-5. *Three horizontal cross-sections of the perturbations applied to the seed logconductivity field in order to arrive to the final conditional logconductivity block in Figure 3-2*

Log conductivity   Perturbation
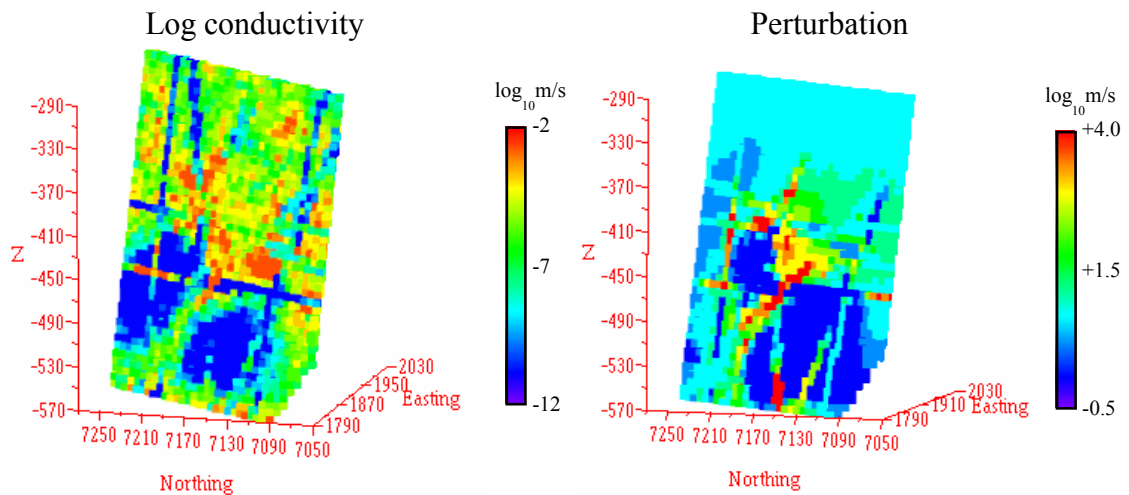
Figure 3-6. *Final logconductivity distribution in fracture #8 and perturbation applied to the logconductivity in the seed field to arrive at the conditional realisation.*

21
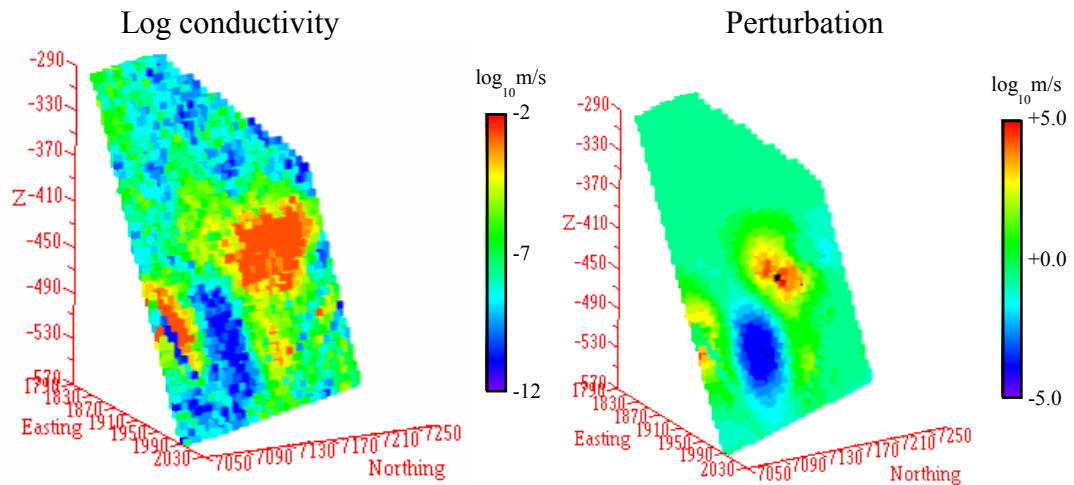
Figure 3-7. *Final logconductivity distribution in fracture #19 and perturbation applied to the logconductivity in the seed field to arrive at the conditional realisation.*
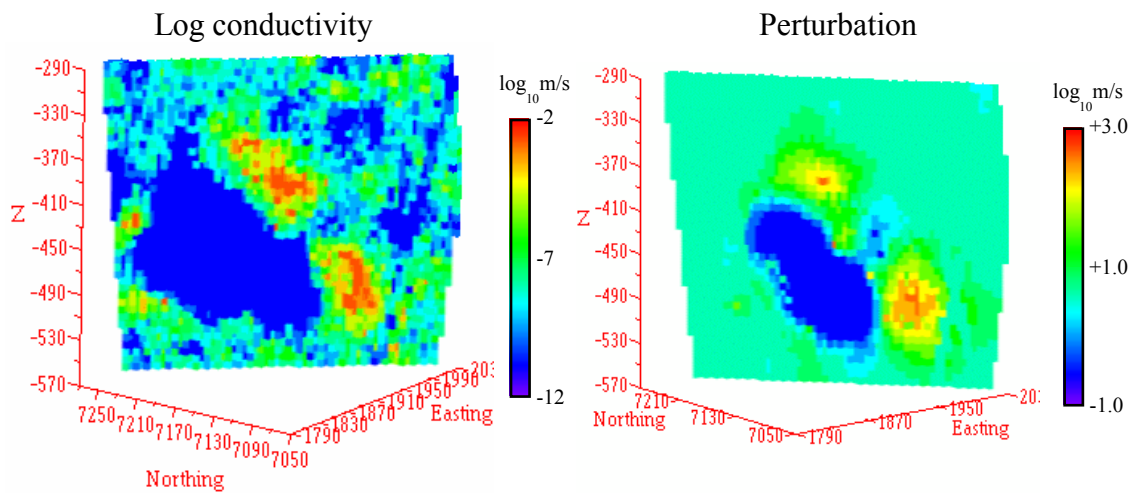
Figure 3-8. *Final logconductivity distribution in fracture #20 and perturbation applied to the logconductivity in the seed field to arrive at the conditional realisation.*

4   Conclusions

It is possible to use stochastic continuum models for the characterisation and modelling of three-dimensional fractured media. Geostatistical and inverse modelling techniques can be used to generate heterogeneous realisations of logconductivity capturing the spatial heterogeneity of conductivities and conditional to structural geology, conductivity measurements and piezometric head measurements. Theoretically, the stochastic nature of the approach could allow uncertainty characterisation through the generation and posterior analysis of multiple realisations, unfortunately, at the moment, uncertainty characterisation is impossible due to computer limitations. The generation of a single realisation conditioned to all information available is very costly.

The process of conditioning to the steady-state and transient piezometric head information is sequential and the evolution of the conductivity field as more data are incorporated could be used to evaluate the relevance of some fractures or the need to consider additional unexplored fractures. The fact that the conditioning process to transient piezometric heads is not capable to match some of the experimental measurements needs to be further explored. It may be due to a weakness of the conditioning algorithm or to some inconsistency between the model and the response sought. An analysis in more detail of why the model cannot be made to reproduce some of the experimental drawdowns must be carried out.

Although in the beginning all fractures in the seed conductivity field are assigned conductivity values with the same means and standard deviations, the conditioning process alters both means and standard deviations and stands out some fractures among the others. Most noticeable fracture #5 increases its average logconductivity from -6.5 to -4.6 $\log_{10}$m/s. The analysis of the evolution of the fracture statistics as the conditioning progresses can also be studied and be helpful in the better understanding of the joint behaviour of the block.

References

Andersson, P., Ludvigsson, J.-E., Wass E., 1998. True Block Scale Project, preliminary characterisation stage, combined interference tests and tracer tests, performance and preliminary evaluation. Äspö Hard Rock Laboratory, International Progress Report IPR-01-44.

Gómez-Hernández, J. J., Sahuquillo, A., Capilla, J. E.. 1987. Stochastic simulation of transmissivity fields conditional to both transmissivity and piezometric data. 1. Theory. Journal of Hydrology, vol. 1-4, no. 203, p. 162-174.

Gentzschein, B., 1997a. Äspö Hard Rock Laboratory. True block scale experiment. Detailed flow logging of core boreholes KA2511A, KI0025F and KA3510A using a double packer system. SKB International Progress Report IPR-01-69, Stockholm, Sweden.

Gentzschein, B., 1997b. Äspö Hard Rock Laboratory. True block scale experiment. Detailed flow logging of core borehole KA2563A. SKB Internal Report, Stockholm, Sweden.

Gentzschein, B., 1998. Äspö Hard Rock Laboratory. True block scale experiment. Detailed flow logging in core borehole KI0023B using a double packer system. SKB Internal Report, Stockholm, Sweden.

Greenbaum, A., 1986. Routines for Solving Large Sparse Linear Systems. Tentacle, Lawrence Livermore National Laboratory, Livermore Computing Center, p 15-21.

Hermansson, J., 1998a. Äspö Hard Rock Laboratory. True block scale experiment. October 1997 structural model; update using characterization data from KA2511A and KI0025F. SKB International Progress Report IPR-01-41, Stockholm, Sweden.

Hermansson, J., 1998b. Äspö Hard Rock Laboratory. True block scale experiment. September 1998 structural model; update using characterization data from KI0023B, SKB International Progress Report IPR-01-42, Stockholm, Sweden.

Hermansson J., Follin S., 1997. Äspö Hard Rock Laboratory. True block scale project. Update of the structural model using characterization data from KA2563A, KA3510A and KA2511A. Scoping stage, SKB Internal Report, Stockholm, Sweden.

Svensson, U., 1997. A site scale analysis of groundwater flow and salinity distribution in the Äspö area. Swedish Nuclear Fuel and Waste Management Co. SKB Technical Report TR 97-17.

Appendix 1: Conditioning logconductivity data

Table A1-1. Co-ordinates and log conductivity conditioning data at those locations in which a fracture has been identified

x(m)	y(m)	z(m)	$\log_{10}K$(m/s)	Fracture
1953.5	7165.1	-389.6	-7.1	#6
1905.6	7248.7	-477.5	-10.7	#6
1946.0	7168.0	-472.8	-11.2	#6
1929.5	7208.5	-462.8	-6.5	#6
1984.3	7186.5	-364.8	-6.3	#7
1949.5	7196.2	-463.5	-8.0	#7
1883.5	7185.1	-488.5	-12.0	#8
1853.9	7167.9	-517.7	-8.0	#9
1863.1	7107.9	-508.4	-7.1	#10
1855.1	7236.5	-507.5	-6.7	#15
1950.1	7162.7	-392.4	-7.0	#16
1929.6	7148.4	-408.9	-11.5	#17
1903.2	7196.5	-469.0	-11.6	#18
1914.2	7185.3	-473.3	-7.6	#18
1880.2	7183.1	-491.7	-10.4	#19
1935.6	7083.5	-500.8	-6.8	#19
1893.7	7154.3	-487.4	-7.7	#19
1936.4	7153.1	-403.4	-9.6	#20
1906.5	7198.4	-465.7	-7.1	#20
1944.3	7153.9	-477.5	-8.1	#20
1916.7	7189.2	-471.6	-7.8	#20

x(m)	y(m)	z(m)	$\log_{10}K$(m/s)

Table A2-2. Co-ordinates and log conductivity conditioning data at those locations in which no fracture has been identified

1980.9	7184.1	-367.6	-8.1
1977.5	7181.7	-370.3	-9.9
1974.0	7179.4	-373.1	-9.5
1970.6	7177.0	-375.8	-8.7
1967.2	7174.6	-378.6	-9.2
1963.8	7172.2	-381.4	-7.8
1960.4	7169.8	-384.1	-9.7
1956.9	7167.4	-386.9	-10.3
1946.7	7160.3	-395.1	-9.0
1943.3	7157.9	-397.9	-9.9
1939.8	7155.5	-400.7	-10.4

1933.0	7150.8	-406.2	-11.3
1926.2	7146.0	-411.7	-10.5
1922.7	7143.6	-414.5	-7.4
1919.3	7141.2	-417.2	-8.8
1915.9	7138.8	-420.0	-8.3
1912.5	7136.5	-422.7	-9.1
1909.0	7134.1	-425.5	-9.0
1905.6	7131.7	-428.2	-9.1
1902.2	7129.3	-431.0	-10.5
1926.2	7209.8	-446.2	-7.9
1922.9	7207.9	-449.5	-9.2
1919.6	7206.0	-452.7	-10.0
1916.3	7204.1	-456.0	-9.3
1913.1	7202.2	-459.2	-9.9
1909.8	7200.3	-462.5	-8.2
1899.9	7194.6	-472.2	-11.6
1896.6	7192.7	-475.5	-9.2
1893.3	7190.8	-478.7	-8.2
1890.0	7188.9	-482.0	-9.8
1886.8	7187.0	-485.2	-12.0
1876.9	7181.2	-495.0	-8.2
1873.6	7179.3	-498.2	-7.6
1870.3	7177.4	-501.5	-9.0
1867.0	7175.5	-504.7	-7.2
1863.7	7173.6	-508.0	-8.0
1860.5	7171.7	-511.2	-10.1
1857.2	7169.8	-514.5	-8.9
1850.6	7166.0	-521.0	-7.9
1847.3	7164.1	-524.2	-9.3
1909.8	7249.7	-475.0	-9.8
1901.4	7247.7	-480.0	-10.1
1897.2	7246.7	-482.5	-12.0
1893.0	7245.6	-485.0	-12.0
1888.7	7244.6	-487.5	-9.0
1884.5	7243.6	-490.0	-12.0
1880.3	7242.6	-492.5	-11.5
1876.1	7241.6	-495.0	-12.0
1871.9	7240.6	-497.5	-10.0
1867.7	7239.5	-500.0	-11.6
1863.5	7238.5	-502.5	-12.0
1859.3	7237.5	-505.0	-11.6
1850.8	7235.5	-510.0	-9.8
1846.6	7234.5	-512.5	-11.7
1842.4	7233.4	-515.0	-12.0
1838.2	7232.4	-517.5	-11.2
1834.0	7231.4	-520.0	-11.1
1926.9	7204.6	-464.6	-8.4
1924.4	7200.8	-466.3	-9.3

1921.8	7196.9	-468.1	-11.8
1919.3	7193.0	-469.8	-11.3
1911.6	7181.4	-475.1	-9.8
1909.1	7177.5	-476.8	-8.3
1906.5	7173.7	-478.6	-9.9
1903.9	7169.8	-480.4	-11.4
1901.4	7165.9	-482.1	-11.6
1898.8	7162.1	-483.9	-12.0
1896.3	7158.2	-485.6	-10.0
1891.2	7150.4	-489.1	-10.3
1888.6	7146.6	-490.9	-10.9
1886.1	7142.7	-492.6	-10.0
1883.5	7138.8	-494.4	-11.4
1880.9	7135.0	-496.2	-11.5
1878.4	7131.1	-497.9	-12.0
1875.8	7127.2	-499.7	-11.2
1873.3	7123.4	-501.4	-9.7
1870.7	7119.5	-503.2	-11.8
1868.2	7115.6	-504.9	-9.4
1865.6	7111.7	-506.7	-7.4
1860.5	7104.0	-510.2	-10.7
1948.9	7191.5	-465.1	-11.1
1948.3	7186.8	-466.6	-11.3
1947.8	7182.1	-468.2	-11.1
1947.2	7177.4	-469.7	-11.4
1946.6	7172.7	-471.3	-11.2
1945.5	7163.3	-474.4	-11.7
1944.9	7158.6	-475.9	-10.6
1943.7	7149.2	-479.0	-11.2
1943.1	7144.6	-480.6	-11.0
1942.6	7139.9	-482.2	-11.5
1942.0	7135.2	-483.7	-10.8
1941.4	7130.5	-485.3	-11.1
1940.8	7125.8	-486.8	-10.7
1940.2	7121.1	-488.4	-11.2
1939.7	7116.4	-489.9	-11.3
1939.1	7111.7	-491.5	-11.1
1938.5	7107.0	-493.0	-11.2
1937.9	7102.3	-494.6	-11.4
1937.3	7097.6	-496.1	-11.2
1936.8	7092.9	-497.7	-9.1
1936.2	7088.2	-499.3	-10.4

Appendix 2: Perturbation of a conductivity realisation

Let $\{K\}=\{K_i, i=1,\ldots,N\}$ represent a realisation of condcutivity over the N numerical cells discretizing the volume of study. This realisation is conditional, by construction, to (n_K) data values, represented by $\{K_m\}=\{K_{im}, i\in(n_T)\}$. Let $\{h\}=\{h_i, i=1,\ldots,N\}$, be the numerical solution of the groundwater flow equation on this realisation, and $\{h_m\}=\{h_{im}, i\in(n_h)\}$, be the set of (n_h) head measurements to which we wish to condition $\{K\}$. The penalty function $F=\sum_{i\in(nh)}(h_i-h_{im})^2$ will not, in principle, be close to zero, indicating that measured heads are not reproduced by the flow simulation in the given conductivity field. In such case, a perturbation $\{\Delta K\}=\{\Delta K_i, i=1,\ldots,N\}$ is added to $\{K\}$ so that the head solution in the updated field $\{K+\Delta K\}$ results in a penalty function close to zero. The perturbation $\{\Delta K\}$ is parameterised as a linear function of the perturbations at a few selected master locations (m) uniformly distributed over the volume of interest. A rule of thumb to select the master locations is to have 1 or 2 master locations per correlation length. The perturbation at any cell i is given by

$$\Delta K_i=\sum_{j\in(m)} \lambda_j \Delta K_j$$

with λ_j computed, within each fracture, by ordinary kriging with the same variogram used for the generation of $\{K\}$. To ensure that conditioning to conductivity is not destroyed by the perturbation, the set of master locations includes the conductivity data locations, i.e., $(m)\supset(n_K)$ and the perturbation at the transmissivity data locations is set constant to zero, $\Delta K_i=0$, $i\in(n_K)$. A non-linear optimisation procedure determines the perturbations ΔK_i, $i\in(m)$ that reduces the penalty function F, close to zero.